Synthesis and optical properties of colloidal germanium nanocrystals

J. P. Wilcoxon, P. P. Provencio, and G. A. Samara
Sandia National Laboratories, Albuquerque, New Mexico 87185-1421
(Received 28 April 2000; revised manuscript received 31 July 2000; published 26 June 2001)

Highly crystalline germanium (Ge) nanocrystals in the size range 2–10 nm were grown in inverse micelles and purified and size separated by high-pressure liquid chromatography with on-line optical and electrical diagnostics. The nanocrystals retain the diamond structure of bulk Ge down to at least 2.0 nm (containing about 150 Ge atoms). One of the objectives of the work was to demonstrate visible light emission from these nanocrystals, and, as it turned out, this dictated emphasis on small ($\lesssim$5 nm) sizes. The background- and impurity-free extinction and photoluminescence (PL) spectra of 2 and 4 nm nanocrystals revealed rich structure which could be interpreted in terms of the band structure of Ge shifted to higher energies by quantum confinement. The sifts ranged from $\sim$0.1 eV to over 1 eV for the various transitions. PL in the range 350–700 nm was observed from nanocrystals 2–5 nm in size. The 2.0-nm nanocrystals yielded the most intense PL (at 420 nm) which is believed to be intrinsic and attributed to direct recombination at Γ. Excitation at high energy (250 nm) populates most of the conduction bands resulting in competing recombination channels and the observed broad PL spectra.

DOI: 10.1103/PhysRevB.64.035417 PACS number(s): 61.46.+w, 78.55.−m

I. INTRODUCTION

The study of semiconductor nanocrystals, or quantum dots, is a very active area of current research, and significant advances are being made in the synthesis and characterization of these interesting materials.[1,2] Particularly interesting has been the influence of quantum confinement on the optical properties of semiconductors as quantum dots are made smaller and smaller. Quantum confinement effects have been studied extensively and are generally well understood in II-VI semiconductors (CdS, CdSe), and to a somewhat lesser degree in III-V semiconductors (GaAs, InP). Success in these two classes of semiconductors has been to a large extent due to the ability to grow, using solution techniques, highly crystalline monodisperse colloidal populations of nanocrystals ranging in size from tens to about 1–2 nm in diameter.[1,2]

There has also been much interest in silicon (Si) and germanium (Ge) nanocrystals, especially in regards to the potential of obtaining useful levels of visible photoluminescence (PL) from these materials. Indeed, visible PL has been observed from both Si and Ge nanocrystals produced by a variety of techniques, most of which grow the nanocrystals in a glass (SiO_2) matrix. These techniques include sputtering,[3–5] laser ablation,[6] sol-gel processing,[7] and ion implantation followed by high-temperature annealing.[8] However, these techniques produce broad distributions of crystal sizes and broad optical absorption and PL features that make definitive interpretation in terms of quantum confinement and other mechanisms difficult. Solution-based synthesis of nanocrystals of these two materials is more difficult than for the compound semiconductors, a factor that has been largely responsible for the lack of highly crystalline monodisperse samples and for the limited progress in characterizing and understanding the properties of these nanocrystals. However, there has been some recent progress in the solution synthesis of these materials,[9,10] raising the prospects for a fuller understanding of the physics.

We have developed a synthesis method based on using inverse micelles as reaction vessels to produce useful quantities of size-selected nanocrystals and have used this method to synthesize a variety of metal, compound semiconductor, and Si nanocrystals.[10–13] These nanocrystals have been remarkable in their monodispersity and the sharpness and richness of their spectral features which have demonstrated strong quantum confinement effects. In this paper we apply this inverse micellar synthesis method to produce size-selected Ge nanocrystals and to study their size-dependent optical absorption and photoluminescence.

In what follows we shall first discuss the synthesis and characterization of our Ge quantum nanocrystals and then present and discuss their optical absorption and PL including comparison with earlier work.

II. SYNTHESIS AND CHARACTERIZATION

Size-selected, Ge nanocrystals were grown by a process which is described in detail elsewhere.[10–13] Controlled nucleation and growth occur in the interior of nanosize surfactant aggregates called inverse micelles. An anhydrous ionic salt (e.g., GeX_4, where X=Cl, Br, or I) is dissolved in the hydrophilic interior of a solution of micelles. The basic idea is that since the ionic salts are completely insoluble in the continuous oil medium used (e.g., octane), nucleation and growth of Ge is restricted to the micelle interior. The interior volume of micelles can be varied over the range of 1–10 nm. We emphasize that the anhydrous salt is dissolved to form a transparent ionic solution but with a complete absence of water; in a sense, the salt is ''hydrated'' by the micelle. The absence of water prevents simple hydrolysis from forming GeO_2, which is why this synthesis must be performed in water-free oils like octane or decane and using a controlled atmosphere glove box. Similarly, the surfactants used, both nonionic aliphatic polyethers or alternatively quaternary ammonium cationic surfactants, must be dissolved in anhydrous tetrahydrofuran (THF) and dried over Na metal or a molecular sieve to remove any small traces of water. Alternatively,

the surfactants may be purified by high-pressure liquid chromatography (HPLC), which results in even better quality, but is more tedious. Once the Ge halide salts are solubilized in the inverse micelles, the formerly clear inverse micelle solution takes on the color of the salt (clear for the Cl salts, light yellow for the Br and I salts). This transparent precursor solution has distinct absorbance peaks much as do charge-transfer complexes of other metal salts (e.g., $CoCl_2$) in water.

We next reduce Ge(IV) to Ge(0) using an anhydrous metal hydride (usually 1 M $LiAlH_4$ in THF). The reduction is rapid with vigorous bubbling as H_2 gas is released, electrons are transferred to the Ge(IV), and the light yellow solution becomes clear (for the smallest clusters formed). One can determine the correct stoichiometry of the reaction by following the disappearance of the Ge(IV) charge-transfer peaks from the precursor solution. Generally we find that for complete reduction we need to use a twofold excess of the $LiAlH_4$ reducing agent. Alternatively, it is possible to effect a four-electron transfer reaction to Ge(IV) using alkaline N_2H_4, but there is the possibility of competing hydrolysis to GeO_2 because of the presence of water. However, our experience is that this hydrolysis is actually slower than the reduction, so either reducing agent is acceptable.

Control over the final cluster size is achieved by a variation of the micelle size, intermicellar interactions, and reaction chemistry. Size-selected Ge clusters with diameters between 2 and ~10 nm were produced. HPLC with on-line spectroscopy, conductivity, and refractive index diagnostics were used to demonstrate 100% reduction of the Ge(IV) to the final Ge(0) nanocrystal form. All reactions took place in anaerobic conditions in a dry box with continuous oxygen and moisture removal. Typical oxygen levels were 0.1 to 1 ppm and moisture levels were 0.5 to 3 ppm in the dry box. All solvents and surfactants used were HPLC grade and were completely dust free. The latter is critical to prevent inhomogeneous nucleation. Since there is no source of oxygen in the reaction mixture, and anhydrous metal hydrides are used as reducing agents, it is possible that the Ge cluster surface is terminated by hydrogen from the metal hydride, although we currently have no direct proof of this. When kept in the glove box under Ar, there appears to be no long term (i.e., 6 month to 1 year) degradation of the Ge nanoclusters.

A HPLC apparatus with automated fraction collection allowed separation of the elution peaks containing the pure Ge nanocrystals without exposure to air or moisture. There are three valuable features of HPLC that helped us determine optimum synthesis conditions: (1) any unreacted salt elutes at a distinct time different from the Ge nanocrystals, (2) any charged species (e.g., salt, ionic surfactants) can be identified by using an on-line conductivity meter, and (3) nanocrystals of different sizes can be separated and their optical properties determined separately on-line, without exposure to oxygen by using size exclusion chromatographic columns. The absorbance spectra were obtained with a bandwidth of 2 nm collecting data from the photodiode array (PDA) every 2 nm and every 2 s of elution time. The photoluminescence and (PL) photoluminescence excitation (PLE) spectra were obtained with a resolution of 1 nm collecting data every 2 nm

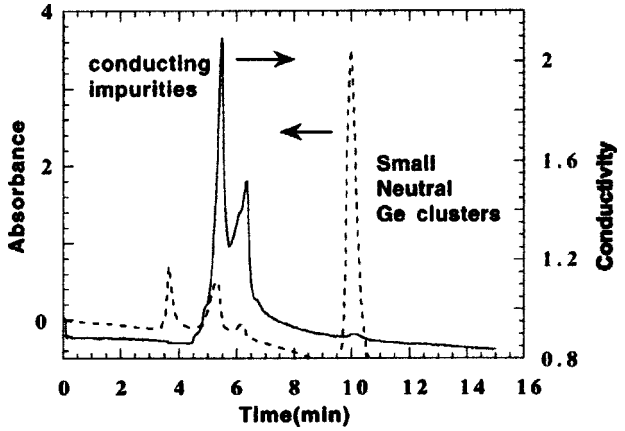

FIG. 1. Coplot of optical absorbance at 250 nm (dashed line) and conductivity (solid line) vs elution time for a reaction mixture of Ge nanoclusters. Chromatography conditions were a Delta-pak^{tm} c 18 (c 18–terminated reverse phase) column with 300-Å pores, using acetonitrile as a mobile phase at 1.0 ml/min flow.

using a SPEX Fluorolog 2, a doubling grating instrument. Symbols shown in the figures are for identification of excitation conditions only. The smooth lines are the actual data obtained under the conditions indicated. The second feature of HPLC analysis is illustrated in Fig. 1 by the separation of Ge nanocrystals made using a nonionic surfactant. We observe that the ionic conducting byproducts of the reaction are separated in time from the small neutral Ge nanocrystals. We note that the elution peak width of these Ge nanocrystals is comparable to the completely monodisperse solvents such as octylamine attesting to the monodispersity of the nanocrystals.[14]

Figure 2 illustrates the separation of two sizes of Ge nanocrystals. Using the PL detector we can identify which size of nanocrystal has significant room-temperature PL, and we can also make sure that no impurity organic chemicals

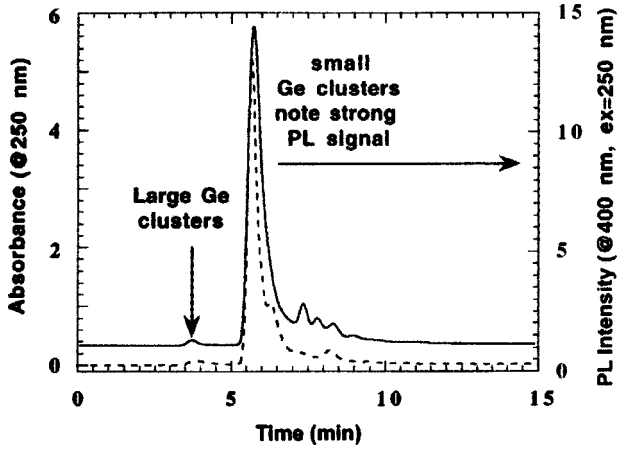

FIG. 2. Coplot of optical absorbance at 250 nm (dashed line) and PL ($em = 400$ nm, excitation, $ex = 250$ nm, solid line) vs elution time for a solution containing two sizes of Ge nanoclusters. Chromatography conditions were a ods200^{tm} c 18 (c 18–terminated reverse phase) column with 120 Å pores, using acetonitrile as a mobile phase at 0.5 ml/min flow.

could be giving rise to the PL signal. Note that the absorbance peak corresponding to the more numerous population of small nanocrystals coincides with a strong visible PL signal. We also obtained the complete absorbance and PL wavelength dependences for each size of the Ge nanocrystal as will be shown in Sec. III.

Inductively coupled plasma/mass spectroscopy (ICP-MS) of the collected Ge fractions showed that nearly 80% of the total Ge was recovered by HPLC, and the only inorganic detected was Ge. Gas chromatography/mass spectroscopy (GC/MS) showed the only significant organic chemical in the collected fractions was the mobile phase solvent. Thus, the fractions are chemically purified by HPLC as desired. In particular, no surfactant was detected. Acetonitrile (ACN) was often the mobile phase solvent. It is an electron donating solvent that passivates the surfaces of the Ge nanocrystals and prevents unwanted aggregation.

An accurate determination of nanocrystal size and size distribution is crucial to understanding the properties of small particles and assessing the influence of quantum confinement. Most methods used to obtain such information have their limitations.[13(b)] We believe that high-resolution chromatography is one of the best techniques and we have recently demonstrated its ability to separate samples that differ in size by as small as 0.2–0.4 nm.[13(b)] Specifically, it was demonstrated that for inorganic nanocrystals in a suitable mobile (solvent) phase, $\ln D_h \sim t_e$, where D_h is the hydrodynamic diameter of the nanocrystal and t_e is the elution time of the cluster. By independent calibration of the chromatographic column with suitable (typically polymer) size standards, the size D_h of the nanocrystals can be obtained from t_e. The width of the elution peak can be compared to monodisperse samples such as organic molecules. Additional width will occur if there is either size or shape polydispersity greater than the resolution limit $\sim$0.2–0.4 nm of the column used to separate the nanocrystals. Since the width of the Ge nanocrystal elution peaks of Figs. 1 and 2 is not greater than that of particle size standards such as C_{60} (fullerene) or even simple molecules like octylamine, we fairly conclude that the size and shape dispersion is under 0.2–0.4 nm, or less than one additional layer of Ge atoms. However, even if this were not the case, the optical spectra are collected every 2 s, which corresponds to a size discrimination of better than 0.2 nm. The spectra shown in the paper do not represent the average spectra through the elution peak, but rather the absorbance and PL spectra at the apex of the elution peak, so size dispersion is not an issue in the spectra shown. Thus, we believe that we know the sizes (certainly the relative sizes) of our samples to better than $\pm$0.4 nm, and the samples are fairly monodisperse.

In addition to the on-line HPLC optical and size characterization discussed above, we used x-ray diffraction (XRD), selected area electron diffraction (SAD), and high-resolution transmission electron microscopy (HRTEM) to examine the Ge nanocrystals. HRTEM lattice fringe images of $d=2$ nm and $d=4$ nm Ge nanocrystals shown in Fig. 3 reveal the high crystalline quality of these clusters.

The largest nanocrystals ($d=8-10$ nm) were collected as a powder after HPLC purification and subjected to x-ray diffraction (XRD) analysis. The diffraction lines are identical to those of bulk Ge (Fig. 4) except for line broadening. Interestingly, no oxide diffraction peaks were observed, though it was not possible to exclude air during the XRD measurement. The SAD reflections on these clusters were also the same as for the bulk, though broadened significantly by the finite crystalline size.

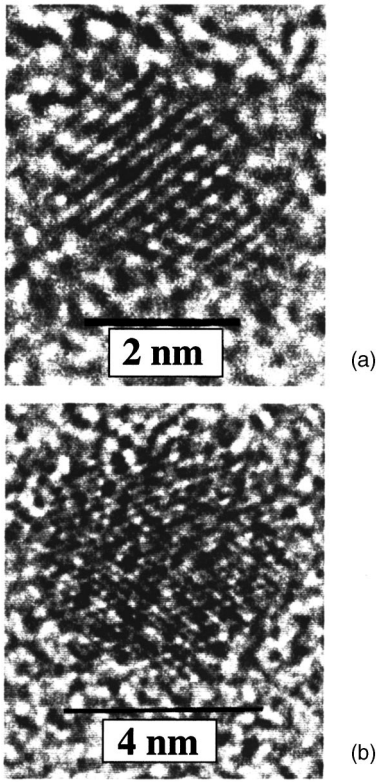

FIG. 3. HRTEM of Ge nanoclusters synthesized by the inverse micelle technique and purified by HPLC.

Although we grew Ge nanocrystals in the size range 2–10 nm, most of the results to be presented are on small (2 and 4 nm) nanocrystals for the following reasons. One of our main

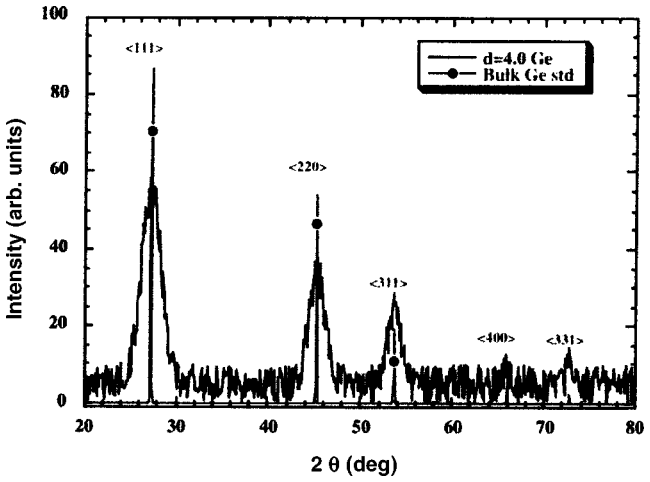

FIG. 4. X-ray diffraction pattern of 4-nm Ge nanocrystals compared with that of bulk Ge.

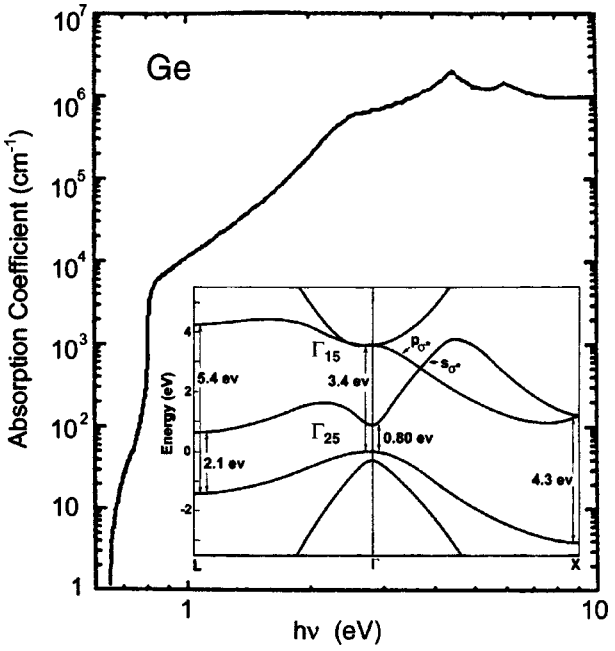

FIG. 5. Measured absorption coefficients near and above the absorption edge of Ge (after Ref. 14). Inset: Band structure of Ge (after Ref. 15).

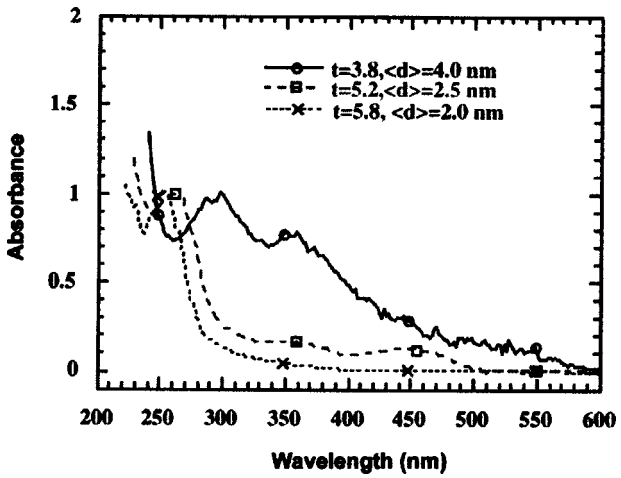

FIG. 6. Influence of nanocrystal size on the absorption spectrum of Ge. The noise in the $d=4.0$ nm spectrum is due to the very dilute concentration of nanocrystals in the sample.

objectives in this work was to look for visible light emission from these nanocrystals, and the small sizes produced sufficiently intense photoluminescence (PL) in this spectral range. The PL from the larger crystals, on the other hand, was weak and generally outside the range (200–800 nm) of our on-line detector. Additionally, the larger nanocrystals lacked some of the sharp spectral features which were important in the interpretation of the results.

III. RESULTS AND DISCUSSION

A. Optical absorption

Before presenting our result on Ge nanocrystals, it is helpful to review the optical absorption of bulk Ge shown in Fig. 5.[15] This absorption reflects a variety of transitions across the Brillouin zone as depicted in the inset.[16] Starting at low energies there is first the broad indirect gap Γ-L absorption followed by the first direct Γ_{25}-Γ_2, absorption at 0.8 eV, followed by a long indirect tail and a shoulder at ~2.4 eV, which may correspond to the first direct transition at L, and then finally cusps at ~4.3 and 6 eV. The cusp at ~4.3 eV is believed to be associated with the direct transition at X.

Bulk Ge has a large dielectric constant (15.4) and small electron and hole effective masses leading to a large excitonic Bohr radius α_B (11.5 nm). This implies that quantum confinement effects should become observable for nanocrystal sizes below this value.

As was true for Si,[10] most of our Ge nanocrystal samples exhibited highly structured optical extinction. Results on three samples are shown in Fig. 6. The $d=2.0$ and 4.0 nm samples came from the same parent solution and are eluted at two distinct times during HPLC separation (see Fig. 2). Thus, differences in their extinction are due to differences in size. The major, smaller size ($d=2.0$ nm) population eluted at 5.8 min and the minor, larger size ($d=4.0$ nm) population eluted at 3.8 min. The sharpness of the elution peaks suggests a narrow size distribution for each population. The third ($d=2.5$ nm) sample was from a different preparation and exhibited a sharp elution peak at 5.2 min. Since the absolute extinction coefficients were not determined sufficiently accurately for all the samples, the spectra in Fig. 6 have been normalized to the extinction at the short wavelength (250–300 nm) peak. This normalization reveals the variation of the shape and shift of spectral features with size. As we shall see below, the various spectral features in the spectra in Fig. 6 can be understood in terms of the electronic structure of bulk Ge blueshifted by quantum confinement and modified by the expected splitting of the bands at Γ_{15}.

Figure 7 compares, over the range 600–250 nm, the extinction spectrum of a $d=4$ nm sample to the absorption spectrum of bulk Ge and to the extinction spectra of Ge nanocrystal samples from the literature as well as a spectrum calculated[9] from Mie theory for $d=6$ nm. Again, since the absolute absorption or extinction coefficients are not known for most of the samples in the figure, the extinction has been normalized (only approximately to keep the curves separated) at the peak near 300 nm. Over the spectral range shown, the distinct features in the bulk spectrum, curve 3 (compare to Figs. 5 and 6), are a shoulder ~550 nm (2.2 eV) associated with the direct band transition at L, and a cusp at 288 nm (4.30 eV) associated with the direct transition at X. The spectrum does not show any clear evidence (although there is a subtle hint) for the direct $\Gamma_{25}-\Gamma_{15}$ transition at ~360 nm (3.4 eV).

The main features in our $d=4.0$ nm nanocrystal spectrum (Figs. 6 and 7, curve 4) are a well-defined shoulder at ~550 nm (2.25 eV) which is essentially not shifted from its counterpart in the bulk spectrum. The lack of influence of quantum confinement on this feature for this size is at present not understood. The next features in curve 4 are peaks at 355 nm (4.5 eV) and 300 nm (4.13 eV), a shoulder at ~280 nm (4.42 eV), and finally a sharp rise in extinction below ~250 nm

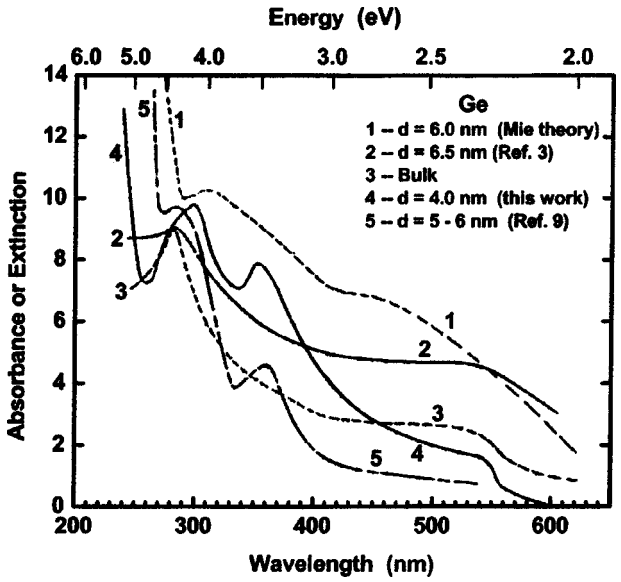

FIG. 7. Comparison of the extinction spectrum of our $d=4$ nm Ge nanocrystals to (i) two spectra from the literature, (ii) the calculated Mie theory spectrum of $d=6$ nm nanocrystals, and (iii) the absorption spectrum of bulk Ge crystal.

(~5 eV). The 355- and 300-nm peaks most likely represent direct transitions from Γ_{25} to the quantum confinement-split conduction bands at Γ_{15}. Reference to Fig. 5 shows that there are two overlapping p_{σ^*} bands for Γ_{15} that are expected to split by quantum confinement as was shown by model calculations for Si.[17] The upper of these two bands for Ge has stronger dispersion (i.e., curvature) than the lower band and is expected to show the larger shift with quantum confinement. Our results are consistent with this expectation. Similar findings have been reported by Heath *et al.*[9] as discussed below.

The fact that the Γ_{25}-Γ_{15} transition is so sharply seen in solution-grown Ge nanocrystals (ours and those of Heath *et al.*) and generally not clearly seen in bulk Ge is interesting. We suggest that its strong emergence in the spectrum of the nanocrystals is a consequence of quantum confinement that enhances the oscillator strength for the transition by mixing states of different k (momentum) values as k is no longer a good quantum number for very small spherical particles. Simply stated, quantum confinement of electrons and holes increases the uncertainty of their crystal momentum, thereby allowing direct optical transitions that normally would require phonon assistance. In bulk Ge the Γ_{25}-Γ_{15} gap is 3.4 eV. The split-off transitions for our $d=4.0$ nm nanocrystals at 3.5 and 4.13 eV suggest a relatively weak (~0.1 eV) quantum confinement effect on the lower and a stronger (~0.7 eV) effect on the higher transition, as expected. Here we should note that both the top of the valence band at Γ_{25} and the conduction bands at Γ_{15} are affected by quantum confinement as predicted by theoretical calculations for Si.[17] Thus, conceivably, and most likely, the lower of the split-off bands at Γ_{15} can actually decrease in absolute energy, but the Γ_{25} band is expected to decrease more leading to the small (0.1 eV) observed blueshift of this Γ_{25}-Γ_{15} transition compared to the bulk transition.

As for the shoulder at ~280 nm in our $d=4.0$ nm spectrum in Fig. 7, it occurs at about the same energy as the cusp in the bulk sample and is probably also associated with the direct transition at X. The situation here is akin to that of the 550-nm transition at L. The close similarity of our nanocrystal spectrum to that of the bulk with respect to both the 500- and 280-nm transitions (spectra 3 and 4 in Fig. 7) is quite remarkable, indicating that scattering does not play a major role in the extinction spectrum of our small nanocrystals. Figure 7 shows that this observation is also true for the data of Heath *et al.*[9] (spectrum 5), and, in fact, spectra 4 and 5 are much more similar to the bulk spectrum (spectrum 3) than to the calculated Mie spectrum and show much less influence of scattering than is suggested by the latter spectrum.

Heath *et al.*[9] synthesized Ge nanocrystals via the ultrasonic-mediated reduction of mixtures of chlorogermanes and organochlorogermanes by a colloidal sodium/potassium alloy in heptane. This solution synthesis approach comes closest to our micellar approach of any of the methods to produce Ge nanocrystals mentioned in Sec. I, and Heath *et al.*'s spectrum for their $d=5-6$ nm sample (spectrum 5 in Fig. 7) is quite similar to ours. Specifically, spectrum 5 exhibits a peak at ~360 nm, a shoulder at ~300 nm, and a second peak at ~285 nm, which correspond closely to the features in our spectrum at 355, 300, and 280 nm, respectively. One difference between our results and those of Heath *et al.* is that they apparently do not see as clear evidence for the transition at 550 nm as we do, although their data in Fig. 7 extends only to ~540 nm.

Also shown in Fig. 7 (spectrum 2) are the results of Hayashi *et al.*[3] for $d=6.5$ nm Ge nanocrystals in SiO_2 produced by rf sputtering. The spectrum resembles that of bulk Ge in that it shows evidence for the transitions at ~550 nm (L point) and ~280 nm (X point), but there is no clear indication of the direct transitions at Γ. The transition features are also broad, reflecting a relatively wide size distribution. Hayashi *et al.* also reported results on samples with smaller nanocrystals and found that the spectrum became essentially featureless for their smallest ($d=2.7$ nm) nanocrystals. However, the onset of extinction shifted to shorter wavelengths with decreasing size in qualitative agreement with our results.

Let us now go back to Fig. 6 and examine the dependences of the spectral features on crystallite size. Consider first the spectrum of $d=2$ nm nanocrystals and compare it to the $d=4$ nm spectrum. The most prominent features in the $d=2$ spectrum are the sharp absorption edge below 300 nm and the peak at 252 nm (4.9 eV). We conjecture that these features are associated with the direct transition from the valence band at Γ_{25} to the upper split-off conduction band at Γ_{15} as argued above for the 300-nm (4.13 eV) peak in the $d=4$ nm spectrum in Fig. 6. This assignment implies for $d=2$ nm a large (~1.5 eV) blueshift of this transition from its bulk value (3.4 eV) due to quantum confinement. This shift is considerably larger than that for Si for the same transition and comparable nanocrystal size[10]—a feature that may be related to the expected larger quantum confinement effect for Ge. In this conjecture, one has to explain the apparent disappearance of the transition to the lower split-off Γ_{15} band for

the $d=2$ nm sample, i.e., the transition corresponding to the 360-nm peak in the $d=4$ nm sample in Fig. 6. This disappearance of this transition for very small sizes may be due to a change in curvature of the lower Γ_{15} band with decreasing size leading to a situation where there are no bound states associated with this band. The spectrum for the $d=2.5$ nm sample in Fig. 6 supports this argument. While in this case we again see a relatively sharp peak and strong quantum confinement associated with the upper split-off Γ_{25}-Γ_{15} transition, the peak corresponding to the lower split-off transition (and to the 360-nm peak in the $d=4$ nm sample) is reduced in intensity to a weak shoulder at about the same energy. This suggests that this feature should vanish at smaller nanocrystal sizes, and this is what is observed for the $d=2$ nm sample.

The increased absorbance (camouflaged by the intensity normalization in Fig. 6) and sharpness of the upper Γ_{25}-Γ_{15} transition with decreasing nanocrystal size is most likely due to the increased influence of quantum confinement and the resulting increase in oscillator strength due to the breakdown of momentum (k) conservation. Quantum confinement could also be responsible for the apparent disappearance of the direct transition at L in the $d=2$ nm spectrum. In this case, the confinement and the zone-folding-like influence of size reduction could lead to large reduction in oscillator strength, and, thus absorbance.

An alternative explanation for the 252-nm peak in the $d=2$ nm spectrum in Fig. 6 may be association with the direct transition at X, which is seen at $\sim$282 nm (4.4 eV) in our larger nanocrystals and in the bulk (Fig. 7), but is blue-shifted due to strong quantum confinement for this small size. (A $d=2$ nm Ge nanocrystal contains only about 190 atoms). However, we note that for the larger nanocrystals (Fig. 7), there is very little evidence for a quantum confinement effect on this transition. If this interpretation were true, then the absorption peaks attributed to the two split-off Γ_{25}-Γ_{15} transitions have vanished for $d=2$ nm. Why these latter transitions would vanish for small nanocrystals is not clear, especially in view of the fact that they are not clearly observed in bulk Ge, but are well-resoled in samples with $d>2$ nm (Figs. 6 and 7). Thus, we favor the first interpretation discussed above.

B. Light emission

Light emission in the IR was observed at room temperature from bulk single crystal Ge long ago.[18] The emission spectrum exhibits two peaks, the first at 1780 nm (0.70 eV) is attributed to phonon-assisted e-h recombination associated with an indirect band gap and the second, more intense peak, at 1520 nm (0.81 eV), is attributed to direct e-h recombination associated with the first direct gap at Γ (i.e., Γ_{25}-$\Gamma_{2'}$). In the present work, our emphasis was on emission in the visible region of the spectrum, and our PL measurements were performed at $\lambda<\sim 800$ nm. All measurements were made at room temperature ($\sim$295 K) with the sample in acetonitrile (ACN) unless otherwise stated.

Figure 8 compares the PL spectra for samples with $d=2$ nm and 4 nm nanocrystals. Also shown are the extinction spectra. This comparison is especially meaningful since both samples came from the same synthesis, but eluted from the HPLC column at different times as shown in Fig. 2. Thus, the differences in spectra (which were taken on-line without exposure to the ambient atmosphere) are primarily due to differences in nanocrystal size. For the $d=4$ nm sample, excitation at 400 nm (3.1 eV) which is below the Γ_{25}-Γ_{15} transitions and above the direct transition at L in energy produces two overlapping emissions with the major peak at 615 nm (2.01 eV) and the minor peak at a shorter wavelength (estimated to be at $\sim$570 nm or 2.2 eV). Comparison of the PL and extinction spectra suggests that the emission (at least the minor peak) may be associated with the absorption edge at L. For the $d=2$ nm sample excitation at 400 nm produces a qualitatively similar PL spectrum but considerably shifted to shorter λ due to quantum confinement. Specifically in this case, the major peak is at $\sim$480 nm (2.6 eV) and the minor peak at $\sim$420 nm (3.0 eV). Again, comparison of the PL and absorption spectra (see also Fig. 7) suggests that the major and minor PL peaks may be associated with direct recombination at Γ (lower split-off band) and L, respectively, although these features are not prominent in the extinction spectra for this sample.

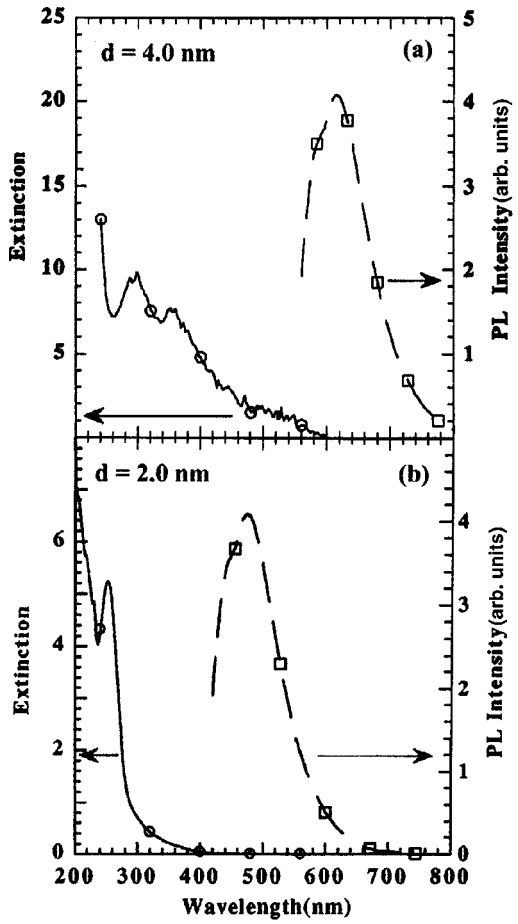

FIG. 8. Extinction and PL spectra of Ge nanocrystal samples with (a) $d=4.0$ nm and (b) $d=2.0$ nm.

If the above assignment of the $\sim$420-nm PL were correct, we observe that excitation at 400 nm, which is at the long λ tail of the absorption edge, excites relatively few electrons to the Γ_{15} conduction band accounting for the relatively low

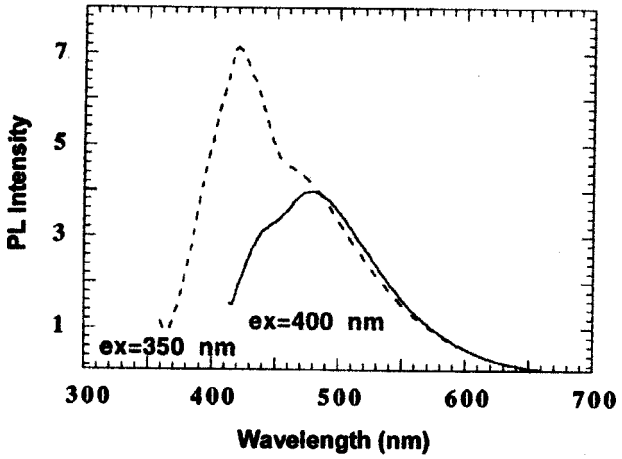

FIG. 9. PL spectra of 2.0-nm Ge nanocrystals for two excitation wavelengths.

intensity of the PL for this transition. To look into this feature further, we investigated a $d \approx 2$ nm sample at two excitation λ's as shown in Fig. 9. Here again, excitation at 400 nm produces essentially the sample PL spectrum as in Fig. 8. However, excitation at 350 nm i.e., above the Γ_{25}-Γ_{15} absorption edge, greatly increases the intensity of what was the minor peak in the spectrum, as would be expected.

The results in Fig. 10 where we explore further the relationship between features in the absorption and PL spectra. These results are from a sample of $d = 2$ nm nanocrystals. Excitation at 400 nm and 350 nm reproduces the same PL spectra as in Fig. 10. Excitation at 300 nm, i.e., at the long λ tail of the upper Γ_{25}-Γ_{15} absorption edge, reduces the intensity of the PL peak attributed (above) to the lower Γ_{25}-Γ_{15} recombination, but produces a distinct shoulder on the short λ side of the PL spectrum. This shoulder is due to a minor PL peak at ~300 nm. Thus, this excitation appears to populate both split-off Γ_{15} bands leading to *e-h* recombination from both. Excitation at 250 nm, i.e., above the absorption peak attributed to the upper $\Gamma_{25} - \Gamma_{15}$ transition, also produces the same shoulder on the PL spectrum as the 300-nm excitation with somewhat lower intensity, but also a second distinct shoulder at ~320 nm.

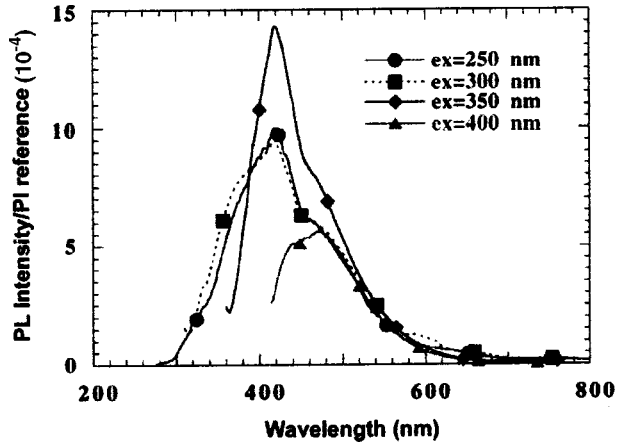

FIG. 10. PL spectra of 2.0-nm Ge nanocrystals for several excitation wavelengths.

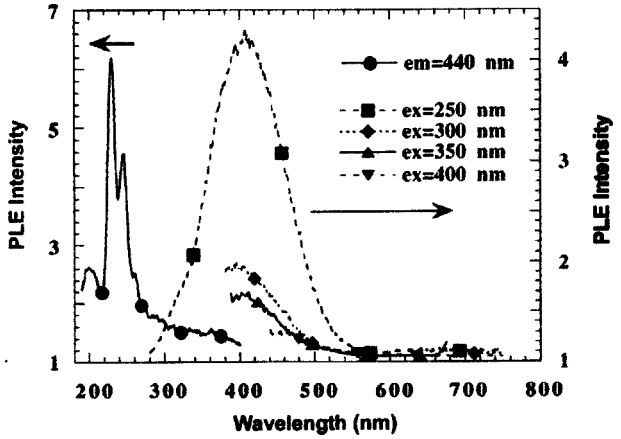

FIG. 11. The PL excitation (PLE) spectrum of 2.3-nm Ge nanocrystals for emission at 440 nm. Also shown are the PL spectra for excitation at different wavelengths.

Clearly then, excitation at these higher energies populates most of the conduction bands across the Brillouin zone, resulting in competing recombination channels and the broad PL spectra shown in Figs. 8–10. Although the above-suggested assignments of the various extinction and PL features are speculative, and thus tentative, what is certain is that these features are not extrinsic, but are attributable to the Ge nanocrystals. Additionally, there is considerable uncertainty in determining the absolute location of a given emission when there are overlapping emission bands in the spectrum. Thus, the above stated λ's (energies) are only approximate.

Figure 11 shows the PL excitation (PLE) spectrum for emission at 440 nm (i.e., on the long λ side of the PL peak) for a sample with $d = 2.3$ nm (eluted at 5.37 mm). The strong absorption in the 250-nm region produces the bulk of this emission. The figure also shows the PL for excitation at 250 nm revealing the same features as in Fig. 10.

It is very difficult to be absolutely certain that extrinsic effects do not contribute to the observed PL, especially in colloidal solutions like our own. Our PL spectra were obtained on-line in our HPLC apparatus, and this approach goes a long way to ensure that we are purifying the samples and measuring the nanocrystals. To further reduce the possibility that the observed PL is caused by contaminants we have been able to transfer the Ge nanocrystals from one solvent to another and study their PL spectra. Figure 12 shows the PL spectra for the same sample and excitation wavelengths as in Fig. 10 in four different solvents of varying polar character (ACN, ethylene glycol, EG, toluene, and ortho-xylene). It is seen that the spectra are essentially identical, except for some changes in intensity. This would, for all practical purposes, rule out the involvement of contaminants unless these contaminants are strongly bound to the nanocrystals' surfaces.

It is useful to compare our PL results to those of other authors. This is done in Fig. 13 where we have plotted the normalized PL intensity versus wavelength. The normalization is arbitrarily done by setting the highest peak intensity

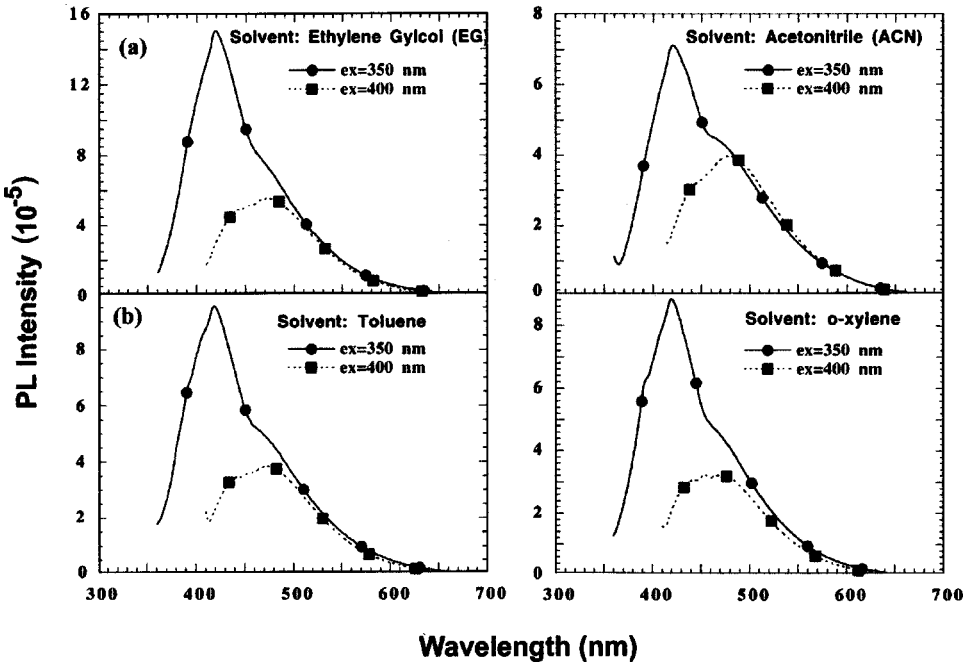

FIG. 12. Comparison of the PL spectra for a $d=2.0$ Ge nanocrystal sample (same as in Fig. 10) dispersed in four solvents of different polar character.

equal to 1.0, and its intent is to allow comparison of the main spectral features. All the spectra in the figure were measured at ~295 K except for the spectrum of Nogami and Abe[7] which was measured at 77 K. The spectra in Figs. 13(a) and 13(b) are for Ge nanocrystals in SiO_2, and the samples are about the same size. The two spectra appear to be similar in overall shape, but the spectrum in 13(b) has better defined long-wavelength features with peaks at ~570 nm (2.18 eV) and ~620 nm (2.0 eV). The higher resolution in this spectrum can be attributed to the fact that it was measured at 77 K. Secondly, the main PL peak of the spectrum in (b) is at ~532 nm (2.33 eV) whereas that for the spectrum in (a) is at ~545 nm (2.28 eV). This difference can be attributed to differences in nanocrystal size as well as the effect of temperature on the band structure of Ge. For example, the indirect band gap of Ge blueshifts by ~0.1 eV between 300 and 77 K and the Γ_{25}-$\Gamma_{2'}$ gap blue shifts by ~0.07 eV over the same temperature range.[15] Actually, the blueshift of the spectrum in (b) relative to that in (a) would have been larger were it not for the fact that the size of the nanoclusters in (b) is somewhat larger. One puzzling aspect of the results in (a) and (b) is that both spectra have about the same overall width, whereas one expects the 77 K spectrum in (b) to be much narrower. We shall comment on the anomalous width of the PL spectra of nanocrystals later in this section.

The main peak at ~540 nm in the spectra in panels (a) and (b) is likely associated with direct *e*-*h* recombination at *L* (Fig. 5). The short decay lifetime (0.9 ns) of this luminescence[4] is consistent with direct recombination. The longer-wavelength PL peaks at 575 and 615 nm may be due to either surface states or to defect levels associated with the gap at *L*.

Figure 13(c) shows the spectrum for our $d=2.2$ nm sample. Overall, the spectrum is much broader than those in panels 13(a) and 13(b), but this is expected (as discussed above) because excitation at 350 nm in our case populates deeper lying conduction bands and opens up more emission channels. In particular, as already discussed in connection with Fig. 9, the peak at ~420 nm in panel 13(c) is probably due to direct Γ_{25}-Γ_{15} recombination. The peak at ~485 nm

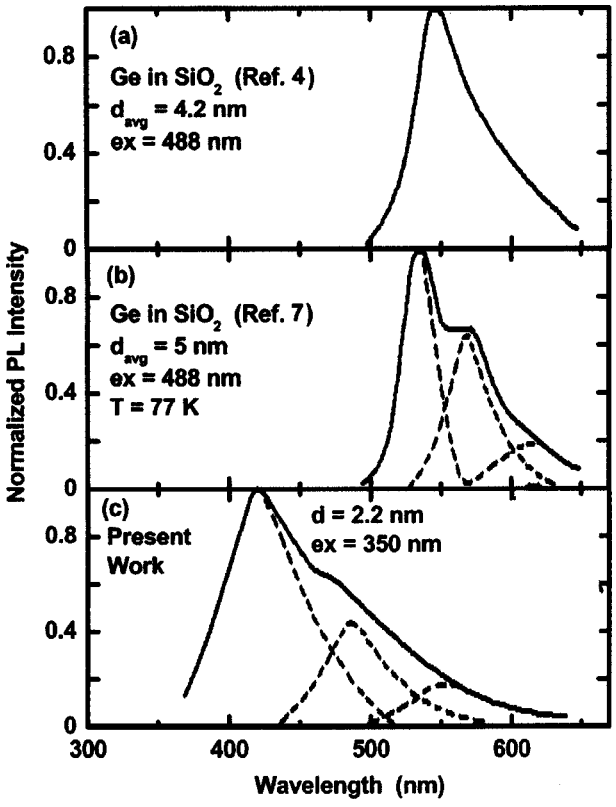

FIG. 13. Comparison of our PL spectra for 2.2-nm Ge nanocrystals with results from the literature for Ge nanoclusters in SiO_2 matrices. The dashed lines represent an approximate decomposition of the spectra into their constituent peaks.

in panel 13(c) appears to correspond to the peak at ~540 nm in panels 13(a) and 13(b) (attributed to direct recombination at L), but shifted to shorter λ due to quantum confinement.

The results summarized in Fig. 13 taken together with the extinction and PL results discussed above provide evidence for quantum confinement effects on the spectral features of our Ge nanocrystals. Recently Zacharias and Fauchet[5] reported luminescence from SiO_2 films containing Ge and GeO_2 nanocrystals. The samples were prepared by dc magnetron sputtering of Ge followed by thermal annealing to crystallize Ge and GeO_2 precipitates. They observed broad PL bands centered around ~400 nm (~2.0 eV) and ~410 nm (~3.0 eV) both of which were independent of the average crystal radius for radii in the range 1.5 to 25 nm. They attribute the blue (3.0 eV) PL to a Ge/O related defect. Clearly, this is very different from our own results where the samples are free of oxygen and an oxide layer.

We now draw attention to the fact that PL spectra of Si (Ref. 4) and Ge nanocrystals are very broad compared to bulk crystals. This is also known to be the case for other semiconductor nanocrystals. Clearly a distribution of nanocrystal sizes can contribute to the width of the spectrum. However, we have also observed that even HPLC-separated samples with narrow elution peaks, which imply narrow size distributions, have broad PL spectra. Furthermore, the breadth does not appear to decrease appreciably with decreasing temperature. Thus, it appears that broad PL peaks are characteristic of nanocrystals. The origin of this feature is not understood at present.

IV. CONCLUDING REMARKS

Using an inverse micellar synthesis, we have successfully grown highly crystalline, size-selected Ge nanocrystals in the 2–10-nm size range. HPLC with on-line optical and electrical diagnostics made it possible to purify and size separately the solution-grown nanocrystals and ensured obtaining background-free extinction and PL spectra. These spectra along with the HRTEM and x-ray- and electron-diffraction data indicated that these nanocrystals retain the bulklike Ge crystal structure down to the smallest sizes grown (2.0 nm diameter containing about 150 Ge atoms). Furthermore, the rich structure in these spectra was interpreted in terms of the electronic band structure of Ge, but shifted by quantum confinement, the shifts ranging from ~0.1 eV to over 1 eV for the various transitions. Photoluminescence in the range ~350 to ~700 nm was observed from clusters 2.0 to ~5.0 nm in size. Most of the observed PL is believed to be intrinsic to the nanocrystals, and several of the peaks were attributed to specific recombination channels. The most intense PL, peaked at 420 nm, was obtained from 2.0-nm nanocrystals and is attributed to direct recombination at Γ. Excitation at high energies (250 nm) populates most of the conduction bands across the Brillouin zone resulting in competing recombination channels and broad PL spectra.

The work presented represents an exploratory study of the influence of size on the optical properties of highly pure Ge nanocrystals and to thereby assess the magnitude of energy shifts attributed to quantum confinement. The strongest evidence for quantum confinement comes from the results for the $d=2$ nm and 4 nm samples in Fig. 8. As noted in the text, these two samples came from the same synthesis and differ only in size. We have tentatively attributed some of the many spectral features in the extinction and PL spectra to specific electronic transitions; however, the assignments are tentative. Much more work is needed to confirm these assignments and to more fully understand the optical properties and electronic structure of these intriguing nanocrystals.

ACKNOWLEDGMENTS

This work was supported by the Division of Materials Sciences, Office of Basic Energy Sciences, U.S. Department of Energy, and by a Laboratory Directed R&D project under Contract No. DE-AC04-AL8500. Sandia is a multiprogram laboratory operated by Sandia Corporation, a Lockheed Martin Company, for the Department of Energy.

[1] See, e.g., MRS Bull. **23** No. 2, 1 (1998), special issue on semiconductor quantum dots.
[2] See also, J. Lumin. **70**, R7-R8 (1996), special issue on nanocrystals.
[3] S. Hayashi, M. Fujii, and K. Yamamoto, Jpn. J. Appl. Phys., Part 2 **28**, L1464 (1989).
[4] Y. Maeda *et al.* Appl. Phys. Lett. **59**, 3168 (1991); **61**, 2187 (1992).
[5] M. Zacharias and P. M. Fauchert, Appl. Phys. Lett. **71**, 380 (1997).
[6] S-T. Ngiam, K. F. Jensen, and K. D. Kolenbrander, J. Appl. Phys. **76**, 8201 (1994).
[7] M. Nogami and Y. Abe, Appl. Phys. Lett. **65**, 2545 (1994).
[8] J. G. Zhu, C. W. White, J. D. Budai, and S. P. Withrow, J. Appl. Phys. **78**, 4386 (1995).
[9] J. R. Heath, J. J. Shiang, and A. P. Alivisatos, J. Chem. Phys. **101**, 1607 (1994).
[10] J. P. Wilcoxon, G. A. Samara, and P. N. Provencio, Phys. Rev. B **60**, 2704 (1999).
[11] J. P. Wilcoxon, R. L. Williamson, and R. J. Baughman, Chem. Phys. **98**, 9933 (1993).
[12] J. P. Wilcoxon and G. A. Samara, Phys. Rev. B **51**, 7299 (1995); J. P. Wilcoxon, P. P. Newcomer, and G. A. Samara, Solid State Commun. **98**, 581 (1996).
[13] (a) J. P. Wilcoxon and S. A. Craft, in *NanoStructured Materials* (Elsevier, New York, 1997), Vol. 9, pp. 85–88; (b) J. P. Wilcoxon, Langmuir **16**, 9912 (2000).
[14] J. P. Wilcoxon, J. E. Martin, and P. P. Provencio, Langmuir **16**, 9912 (2000).
[15] See, e.g., S. M. Sze, *Physics of Semiconductor Devices* (Wiley Interscience, New York, 1969), Chap. 2 and references therein.
[16] M. L. Cohen and T. K. Bergstresser, Phys. Rev. **141**, 789 (1966).
[17] M. V. Rama Krishna and R. A. Friesner, J. Chem. Phys. **96**, 873 (1992).
[18] J. R. Haynes, Phys. Rev. **98**, 1866 (1955).